

# Liquid Plug Dynamics in Microfluidic Flexible Channels – a Small Airway Model

Ying Zheng<sup>1</sup>, Hideki Fujoka<sup>1</sup>, Yusuke Torisawa<sup>1</sup>, Shuichi Takayama<sup>1,2</sup>, James B. Grotberg<sup>1</sup>

<sup>1</sup>Department of Biomedical Engineering, <sup>2</sup>Department of Macromolecular Science and Engineering, University of Michigan, Ann Arbor, MI

## INTRODUCTION

Chronic obstructive pulmonary disease is the fourth leading cause of death in America with characteristics of airflow obstruction, airway closure and airway wall remodeling. Liquid plugs can form due to interfacial instability, airway wall collapse or a combination of both. The propagation of a formed plug can produce high pressure, high shear stress, and large gradients of each, which may damage the cells lining the wall (Fujioka and Grotberg, 2004; Zheng, 2007).

This study is motivated by an interest in the effect of wall flexibility on the plug propagation and its resulting wall stresses in small airways. Cell injuries have been investigated experimentally during airway reopening in Gaver's group (Bilek, 2003; Kay, 2004) by propagating the semi-infinite air bubbles through a rigid chamber lined with airway epithelial cell and in Huh et al. (Huh, 2007) of liquid plug propagation and rupture on human airway epithelial cells lined microengineered airway system. Fluid stress and stress gradients on the rigid walls during the two phase flow has been demonstrated to be responsible for the cell injuries in these experiments. Understanding is needed on the plug dynamics and wall stresses in flexible channels to mimic the real physiologic situations.

## METHODS AND PROCEDURES

Experiments: The flexible microchannel is made by two layers: main channel layer, which is fabricated with soft lithography method using materials of PDMS at a curing ratio of 10:1; and a thin membrane layer with thickness of 5-7  $\mu\text{m}$ , which is spin-coated on

a silanized clean glass cover slide. The channel dimensions are around 100 $\mu\text{m}$  in height and 100 $\mu\text{m}$  in width. The two layers were sealed against each other using a plasma oxidizer (11005-plasma Prep II, SPI, West Chester, PA). The microchannels were filled with the liquid. The inlet and outlet are connected to reservoirs which were open to the atmosphere. A pair of air bubbles was injected in the liquid to form a plug, which propagated with a specified pressure from the gravity pump. A CCD camera (Hamamatsu Orca-100), connected to an inverted fluorescent microscope (TE-300, Nikon, Tokyo, Japan), and SIMPLE PCI software (Compix Inc.) were used to record the plug motion and wall deformation.

Mathematic Model:

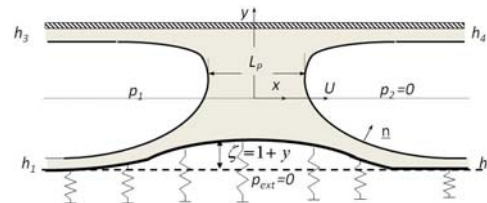


**Figure 1.** Schematic of propagation of liquid plug with length  $L_p$  in flexible channel with speed  $U$  and driven by the pressure drop  $p_1-p_2$ .

The steady plug propagation is numerically simulated in a 2-D channel with top wall rigid and bottom wall flexible, shown in Figure 1. The flow governing equations are  $\nabla p = \nabla^2 \underline{u}$ ,  $\nabla \cdot \underline{u} = 0$ . On the flexible wall, the fluid stress balances with the wall tension:  $T_L \kappa_{LW} - f(\zeta) = -C \underline{n}_w \cdot \underline{T} \cdot \underline{n}_w$  in which,  $T_L$  is the longitudinal tension scaled with the surface tension;  $\zeta(x) = l + y$  is the lower wall deformation with undeformed wall  $\zeta(x) = 0$ ;  $f(\zeta)$  is the nonlinear spring tension with respect to the wall deformation, obtained by fitting the pressure-deformation curve

measured in the experiments with the formula  $f(\zeta)=A\zeta^3 + B\zeta$  where  $A=76.8$  and  $B=0.13$ . The wall damping and inertia are neglected in the wall equation due to the fact of thin flexible membrane and Stokes flow regime. The curvilinear computational grid was generated from two dimensional Poisson's equation. SIMPLER algorithm is used to solve momentum and pressure equations. The wall equation is solved using Newton's method.

## RESULTS

The wall deformation is observed during plug propagation for different plug length and propagation speed. Figure 2 shows the plug dynamics and wall deformation for 3 different situations of plug length and speed.

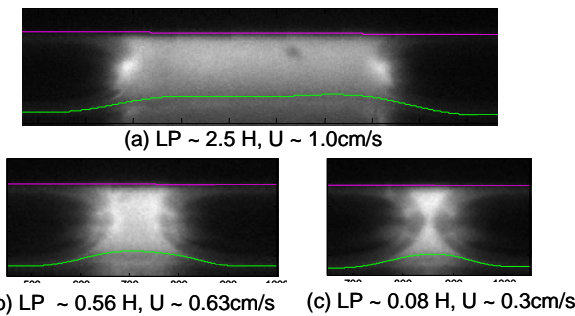


**Figure 2.** Instantaneous flexible wall deformation during plug propagation. H is the channel height, which is about 100 $\mu$ m.

Image analysis was performed to extract the wall shape and quantify the wall deformation. The maximum wall deformation for the three cases shown in Figure 2 is measured to be (a)  $15.5 \pm 1\mu$ m, (b)  $12.5 \pm 1\mu$ m, and (c)  $11 \pm 1\mu$ m. It shows to increase with increasing plug length and speed. The average strain along the wall, defined as the arc length difference normalized by the original wall length, is measured to be (a) 0.7% (b) 1.0% and (c) 1.2%, which increases with decreasing plug length and speed.

The plug flow pattern is calculated as shown in Figure 3 with the fluid stress and stress gradients comparing the flexible wall and rigid channel walls.

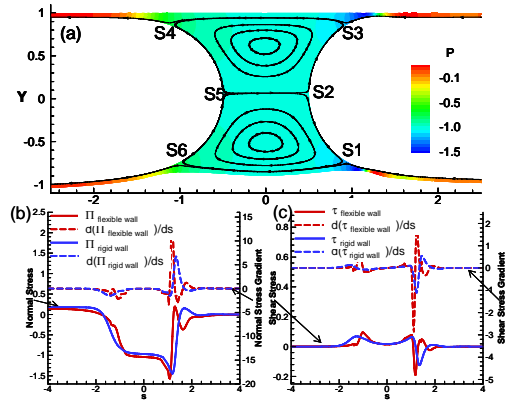


**Figure 3.** (a) The plug flow patten with pressure contour and flow streamlines at  $Ca=0.01$ ,  $LP=1$ ,  $Re=0$  and  $T_L = 1$ . (b) Normal fluid stress and stress gradients along x direction (c) Shear stress and stress gradients from the fluid along x direction.

The maximum flexible wall deformation is measured to be around 10% of the channel width at this parameter set, which is in the same order as what we measured in the experiment (11-15%). The normal stress shows little changes with wall flexibility but the normal stress gradient has a larger peak for the flexible wall. Shear stress and its gradient increases largely on flexible wall, which increases the risk on the cell damages during diseases like emphysema.

## SUMMARY

We experimentally observed the flexible wall deformation during plug propagation and numerically predicted high stress and stress gradients due to the increase of wall flexibility. Diseases like emphysema may cause more cell/tissue damages during airway reopening process.

## REFERENCES

- Fujioka H and Grotberg JB (2003). *J Biomch. Eng.*, 126: 567-577.
- Zheng Y et al (2007). *Phys. Fluids*, 8,082107.
- Bilek AM et al (2003). *J App Physio.*, 94: 770-783.
- Kay SS et al (2004). *J App Physio.*, 97: 269-276.
- Huh D et al (2007). *PNAS*, 104: 18886-18891.

## ACKNOWLEDGEMENTS

This work is supported by NIH Grant Nos. HL84370, HL41126, and HL64373, and NASA Grants No. NAG3-2740 and NNC04AA21A.